Spin-state stability in Mn_2O_3 across the volume collapse phase transition under pressure up to 41 GPa

V. Balédent ⬤

Université Paris-Saclay, CNRS, Laboratoire de Physique des Solides, 91405 Orsay, France

S. R. Shieh

Department of Earth Sciences, University of Western Ontario, London, Ontario N6A5B7, Canada

J.-P. Rueff ⬤ *

Synchrotron SOLEIL, L'Orme des Merisiers, Départementale 128, 91190 Saint Aubin, France
and *Laboratoire de Chimie Physique-Matière et Rayonnement*, CNRS, UMR 7614,
Sorbonne Université, 4 Place Jussieu, 75252 Paris, France

We investigate the spin state stability of Mn in α-Mn_2O_3 through the structural, insulator-to-metal transition under high pressure by x-ray emission spectroscopy (XES) and x-ray diffraction (XRD) up to 41 GPa. The XES spectra show a broadening of the main line and a weak shift of the satellite feature as pressure increases but no signature of spin transition while XRD confirms the full conversion to the *Cmcm* phase at high pressure. Using multiplet calculations, we suggest that the XES spectral changes under pressure is driven by the increased Coulomb interaction in the compressed lattice. The absence of spin transition through the phase transition could be caused by Jahn-Teller distortions on the Mn sites, which stabilize the spin state, possibly leading to hopping conductivity owing to polaronic effects.

I. INTRODUCTION

Manganese oxides have garnered large interest in various physicochemical applications in view of their unique structural, chemical, electronic, or magnetic properties owing to the multiple oxidation states, redox properties, site symmetry, or spin state, which Mn can adopt [1–5]. Among these oxides Mn_2O_3 has attracted special attention as a magnetic semiconductor with potential interest for catalysis, energy storage as electrode materials [6], magnetic data storage [7], or water treatment [8]. Investigating the structural or magnetic stability in highly constraint environment is therefore a key aspect for potential applications.

The pressure-temperature structural phase diagram of Mn_2O_3 has been studied by Ovsyannikov *et al.* [9] using x-ray diffraction and electron microscopy. Starting from α phase at ambient conditions, Mn_2O_3 adopt different perovskite-like structural variants while transforming to Mn_3O_4 at temperatures above 1200 K. From the electronic perspective, which is the focus of the present study, Hong *et al.* [10] have investigated more recently the phase transition of α-Mn_2O_3 under high pressure up to 45 GPa at room temperature. Mn_2O_3 is insulator at ambient pressure, prone to semiconductor behavior, with a cubic structure in the *Ia*-3 space group and a high-spin (HS) $3d^4$, $S = 2$ configuration. Using x-ray diffraction and transport measurements, the authors revealed

a phase change from the cubic phase to an orthorhombic phase with the space group *Cmcm* around $P_c = 20$–25 GPa. The transition features a significant contraction of the volume of $\sim$12%. Simultaneously, Mn_2O_3 exhibits a strong decrease of resistivity leading to a metal-like behavior at higher pressures.

The combined structural and insulator-to-metal transition was suggested to arise from a spin-state transition, from high spin to low spin (LS), which has been widely studied in transition-metal oxides under pressure [11–15]. HS-LS transition indeed is associated with a collapse of the atomic volume because of the spin rearrangement, which could be responsible for the volume contraction observed in Mn_2O_3, possibly leading to a delocalization of the $3d$ electrons as observed in Fe_2O_3 [16]. However, no supporting evidence has been reported to date yet.

In this article, we report the investigation of the spin transition in Mn_2O_3 under high pressure by high-resolution, synchrotron-based x-ray emission spectroscopy (XES) at the Mn Kβ line. XES appears well adapted to this study as a well-established probe of the local spin state and metal–ligand interaction of $3d$ metal, and more specifically of Mn compounds [17–22], compatible with high-pressure sample environment. Our results demonstrate that the spin state remains stable through the volume collapse, insulator-metal transition. The effect is ascribed to Jahn-Teller distortions on the Mn sites, which stabilize the HS state and the possible interplay of polaronic effects.

---

*Contact author: jean-pascal.rueff@synchrotron-soleil.fr

II. EXPERIMENTAL RESULTS

A. Methods

The experiment was performed at the GALAXIES beamline at SOLEIL synchrotron. The incident x-ray coming from the U20 in-vacuum undulator is monochromatized by a liquid nitrogen-cooled Si(111) double crystal monochromator and focused onto the sample in a $30 \times 80 \, \mu m^2$ spot using a toroidal mirror. The XES spectra were measured using the beamline multi-analyzers scanning spectrometer "MULTIXS" laid out in the Rowland circle geometry. The spectrometer was equipped with two Si(110) spherically-bent crystal analyzers with 1 m bending radius that were operated around the Bragg angle of 84.2 deg corresponding to the nominal energy of Mn $K\beta$ line maximum at 6490.4 eV. We used a silicon drift diode (SDD) as detector. The overall spectrometer resolution was estimated at 1.1 eV as deduced from the full width at half maximum (FWHM) of the elastic line.

High purity Mn_2O_3 powder from SigmaAldrich (99.9% purity) was loading in a diamond anvil cell (DAC) with silicone oil as pressure transmitting medium to keep the experimental conditions as close as possible to Ref. [10]. Ruby chips were inserted for *in situ* pressure calibration. The DAC was equipped with 300-μm culet size diamonds and a Re gasket used as sample chamber. The gasket hole was 150 μm in diameter with an initial thickness of 30 μm after preindentation. The pressure was estimated from the ruby fluorescence method [23].

The XES spectra were recorded in transmission geometry through the diamonds at an incident photon energy of 10 keV and a scattering angle of 15 deg by scanning the XES spectrometer energy in the 6465–6510 eV range with 0.25 eV step.

To confirm the structural change, we performed high pressure x-ray diffraction (XRD) at selected pressures in parallel to the XES measurements by moving the pressure cell to the laboratory-based XRD diffractometer installed at Laboratoire de Physique des Solides. The diffractometer utilizes a microfocused Mo tube ($\lambda = 0.71$ Å) equipped with a Montel multilayer focusing optics providing a beam size of 100 μm at the sample with a divergence of 0.5 mrad. The diffracted intensity is collected by a 2D MAR345 detector and radially integrated to obtain the diffraction pattern. Note that the angular range is limited to a maximum of $2\theta = 25$ deg because of the DAC aperture. For each pressure, the exposure time was 30 minutes.

B. XES results and diffraction

Figure 1 shows the measured Mn $K\beta$ XES spectra as a function of the applied pressure. The spectra were aligned to the $K\beta$ line maximum at 6490 eV and normalized in intensity after subtraction of a linear background. The spectra are consistent with Mn_2O_3 Mn $K\beta$ XES ambient pressure spectra reported elsewhere [18,19,24,25]. The spectra consist of an intense main line and a well-defined satellite on the low-energy side usually referred to as $K\beta_{1,3}$ and $K\beta'$, respectively. No noticeable changes are observed under high pressure except a slight broadening of the $K\beta_{1,3}$ main line and a weak displacement of the $K\beta'$ satellite toward high energy (see inset in Fig. 1). The spectra are conformed to
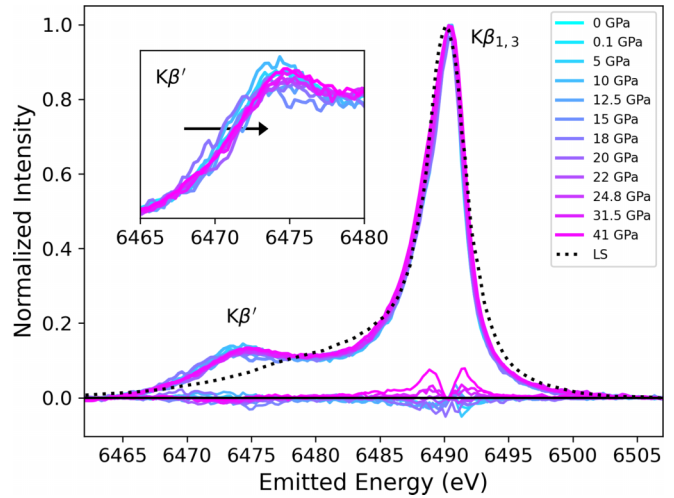

FIG. 1. Mn_2O_3 $K\beta$ XES spectra as a function of pressure up to 41 GPa (solid lines). The difference spectra with respect to ambient pressure are shown at the bottom. The inset is a zoom on the satellite region with the arrow indicating the trend as pressure increases. The MnTe spectrum from Ref. [26] shown with dotted line is indicative of a LS state.

the spectral shape for a Mn^{3+} HS configuration. Especially, the high-pressure spectra above 25 GPa clearly depart from a typical Mn LS configuration spectrum, which is marked by a strongly reduced satellite intensity [17,18,26] even though the sample is already in the HP phase. To ease the comparison, we have added the LS spectrum measured in MnTe at high pressure from Wang *et al.* [26] as dotted line in Fig. 1.

The structural changes is confirmed by the XRD patterns shown in Fig. 2. The patterns were refined using the LP *Ia*-3 and HP *Cmcm* space groups. Our XRD data confirm that Mn_2O_3 has adopted the HP structure near 28.8 GPa with a volume proportion of $87 \pm 5\%$, in good agreement with previous studies [10,27]. The proportion is estimated from the
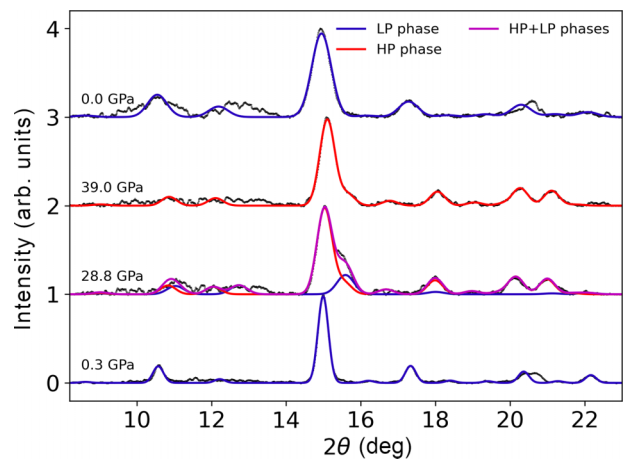

FIG. 2. XRD patterns of α-Mn_2O_3 with increasing pressures from bottom to top (dots). The top diffraction pattern refers to measurement obtained from pressure quench. The refinements within the LP or HP space groups are indicated as blue (LP) and red (HP) lines. In the case of coexistence at 28.8 GPa, the sum of the two contributions is indicated by the magenta line.
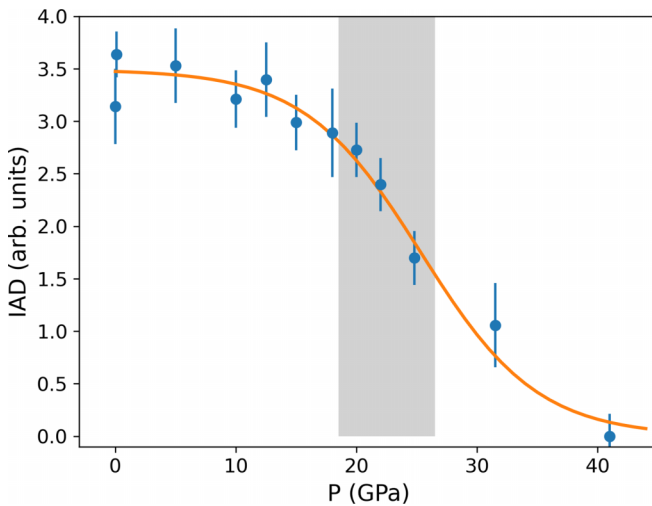
FIG. 3. Computed IAD values from the difference spectra (circles). The data is fitted by an sigmoidal function (solid line). The shaded area indicates the structural coexistence region as reported in Ref. [10].

TABLE I. Parameters used in the multiplet calculations. The valued of the F and G Slater integrals are expressed in terms of scaling factor with respect to the nominal atomic value.

	Site sym.	Spin state	$10Dq$ (eV)	F_{pd} (%)	G_{pd} (%)
LP	$D4h$	HS	2.24	22	66
	$D3h$	HS		22	66
HP	$D4h$	HS	3.10	40	66
	$D3h$	HS		40	66

ratio between the intensity of the HP peak at 15.03 deg and the LP peak around 15.55 deg. At this pressure the refined lattice parameters are $a = 9.13 \pm 0.03$ Å for the cubic LP phase and $a = 2.76 \pm 0.03$ Å, $b = 9.13 \pm 0.03$ Å, and $c = 6.82 \pm 0.03$ Å for the orthorhombic HP phase corresponding to a volume of 31.2 ± 0.3 cm^3/mol and 25.9 ± 0.2 cm^3/mol, respectively, in agreement with previously reported values. The LP phase content decreases upon further compression until 39 GPa where the diffractogram exhibits only the HP phase with lattice parameters of $a = 2.73 \pm 0.01$ Å, $b = 9.08 \pm 0.02$ Å, and $c = 6.76 \pm 0.02$ Å corresponding to a volume of 25.3 ± 0.2 cm^3/mol.

The amplitude of the XES spectral changes can be better visualized using the integrated absolute difference (IAD) method. The IAD value is deduced from the integrated intensity of the difference spectra—represented at the bottom of Fig. 1. Although based on relative scale, the IAD can help to monitor the evolution of the spin state with pressure or other external parameters [22,28,29]. The variation of the IAD value with pressure is shown in Fig. 3. The IAD shows a s-shape behavior with pressure characterized by a flex point around 20–25 GPa where the structural/resistivity change were initially observed [10]. To pinpoint the pressure more precisely, the IAD values were fitted by a sigmoidal function and our results suggest the transition pressure is around 25 GPa.

III. DISCUSSION

While no spin transition is observed, the XES spectra show a systematic, yet weak, broadening of the main line with pressure and a shift of the satellite peak toward high energy. To capture the origin of these effects, we performed multiplet calculations of the XES spectra. The calculations were performed using the CRISPY software [30] starting from HS Mn^{3+} configurations both in $D4h$ and $D3h$ symmetries with a respective weight of 1/4 and 3/4 to reproduce the Mn sites distribution in the LP structure. The $D4h$ site symmetry was considered instead of Oh to take into account the distortion

of the Mn sites owing to Jahn-Teller effects as reported in Ref. [9] and other Mn perovskites [31]. The starting parameters (crystal field splitting $10Dq$, Coulomb interaction F_{pd} and exchange interaction G_{pd}) in the final state were derived from the calculations reported in Hwang *et al.* [25] for Mn$_2$O$_3$. The two other crystal-field parameters in the $D4h$ symmetry Ds, Dt were fixed at 0.1 eV. The G_{pd} scaling factor was further reduced to 66% to obtain the correct energy splitting between the main line and the satellite. As in Ref. [25], charge transfer hybridization effects were not included. The optimized parameters are summarized in Table I for both LP and HP states. When transitioning from the LP to the HP phase, we expect $10Dq$ to increase as the Mn-O distances shorten. A rough estimate based on XRD suggests an increase from 2.24 eV to 3.1 eV as pressure rises from 0 to 40 GPa. Furthermore, the 3p-3d Coulomb interaction F_{pd} was increased from 22% to 40%, which we relate to the stronger orbital overlap as pressure increases. We applied the same scheme to the calculations within the $D3h$ site symmetry. Note that in the $D4h$ symmetry, the Mn spin state remains in the HS configuration independently from $10Dq$ while it would change from HS to LS in the Oh symmetry, leading to significant spectral changes that are not observed experimentally (see the Supplemental Material [32]).

The LP and HP experimental and simulated spectra are presented in the top and bottom panel of Fig. 4, respectively. The simulated spectra reproduce fairly well the main line but not for the satellite features with a double peak instead of a single, broad peak. Such a discrepancy were found earlier [25] revealing the limitations of the multiplet calculations to describe the Kβ XES process. Our intention, however, is to capture the effects of pressure on the spectral shape. As shown in the bottom panel of Fig. 4, the simulated spectra succeed in reproducing both the broadening of the main line and the shift of the satellite, which confirms that the increase of the F_{pd} Slater integral likely drives the spectral changes. In this view, the s-shape IAD curve reflects the volume discontinuity reported by [10] at P_c, which translates into an step-like change of the Coulomb interaction via the shortening of the metal-ligand bond length.

Our study further illustrate the complexity of the electronic properties of Mn$_2$O$_3$ and more generally of perovskite manganites as resulting from a strong interplay between electronic, spin, and lattice degrees of freedom, and leading to intricate phenomena such as spin-induced ferroelectricity [7], oxygen driven anisotropic transport [33,34], or colossal magnetoresistance [35]. Apart from our XES results pointing to the absence of spin transition, there is no direct
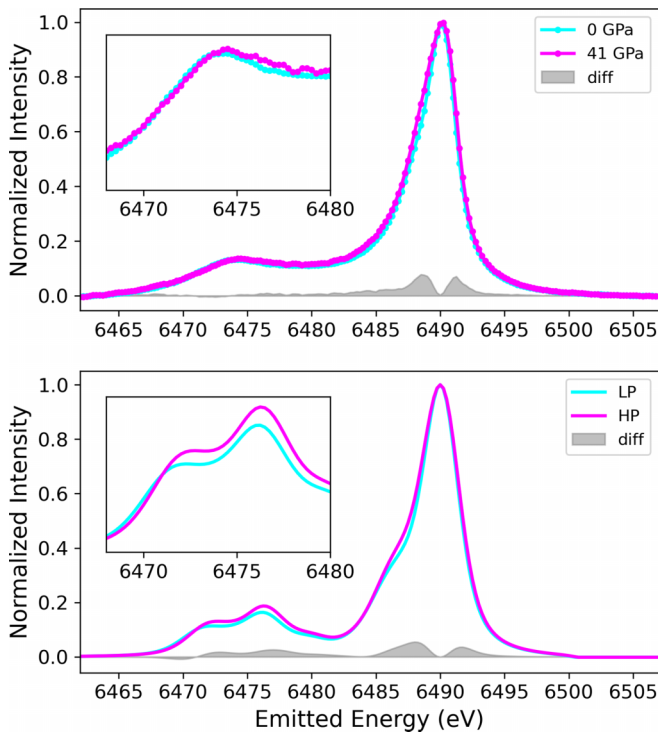
FIG. 4. Experimental spectra measured at 0 and 41 GPa (top panel) and simulated spectra for low-pressure and high-pressure regimes (bottom panel). For comparison purpose, the spectra were normalized to the maximum intensity; the HP-LP spectral differences are indicated by the gray-shaded areas.

determination so far of the Mn magnetic moment in the *Cmcm*, postperovskite phase of Mn_2O_3 at high pressure. The magnetic stability could indicate that the $3d$ electrons remain partly localized at high pressure, with a possible role of the O-p bandwidth to stabilize the spin state under pressure [13]. In this picture, the insulator-metal transition itself could be rooted in the hopping conductivity owing to polaronic effects in presence of octahedral tilting, Jahn–Teller distortion, and partial charge ordering, which are commonly found in manganite perovskites [9].

IV. CONCLUSIONS

In conclusion, we successfully investigated the spin transition in Mn_2O_3 under pressure through the insulator-metal transition by x-ray emission spectroscopy. Our XES results demonstrate the stability of the spin state through the transition while the spectral changes can be interpreted by the increase of the p-d Coulomb interaction at high pressures. The combined spin stability and insulator-to-metal transition is ascribed to effects of Jahn-Teller distortions on the Mn sites and hopping conductivity owing to the polarons.

[1] M. V. J. M. D. Coey and S. von Molnár, Mixed-valence manganites, Adv. Phys. **48**, 167 (1999).

[2] T. Kimura, T. Goto, H. Shintani, K. Ishizaka, T. Arima, and Y. Tokura, Magnetic control of ferroelectric polarization, Nature (London) **426**, 55 (2003).

[3] M. Rini, R. Tobey, N. Dean, J. Itatani, Y. Tomioka, Y. Tokura, R. W. Schoenlein, and A. Cavalleri, Control of the electronic phase of a manganite by mode-selective vibrational excitation, Nature (London) **449**, 72 (2007).

[4] K. Lai, M. Nakamura, W. Kundhikanjana, M. Kawasaki, Y. Tokura, M. A. Kelly, and Z.-X. Shen, Mesoscopic percolating resistance network in a strained manganite thin film, Science **329**, 190 (2010).

[5] C.-H. Kuo, W. Li, L. Pahalagedara, A. M. El-Sawy, D. Kriz, N. Genz, C. Guild, T. Ressler, S. L. Suib, and J. He, Understanding the role of gold nanoparticles in enhancing the catalytic activity of manganese oxides in water oxidation reactions, Angew. Chem., Int. Ed. **54**, 2345 (2015).

[6] N. F. M. Yusoff, N. H. Idris, M. F. M. Din, S. R. Majid, N. A. Harun, and M. M. Rahman, Investigation on the electrochemical performances of Mn_2O_3 as a potential anode for Na-ion batteries, Sci. Rep. **10**, 9207 (2020).

[7] J. Cong, K. Zhai, Y. Chai, D. Shang, D. D. Khalyavin, R. D. Johnson, D. P. Kozlenko, S. E. Kichanov, A. M. Abakumov, A. A. Tsirlin *et al.*, Spin-induced multiferroicity in the binary perovskite manganite Mn_2O_3, Nat. Commun. **9**, 2996 (2018).

[8] J. Cao, Y. Zhu, L. Shi, L. Zhu, K. Bao, S. Liu, and Y. Qian, Double-shelled Mn_2O_3 hollow spheres and their application in water treatment, Eur. J. Inorg. Chem. **2010**, 1172 (2010).

[9] S. V. Ovsyannikov, A. M. Abakumov, A. A. Tsirlin, W. Schnelle, R. Egoavil, J. Verbeeck, G. Van Tendeloo, K. V. Glazyrin, M. Hanfland, and L. Dubrovinsky, Perovskite-like Mn_2O_3: A path to new manganites, Angew. Chem., Int. Ed. **52**, 1494 (2013).

[10] F. Hong, B. Yue, N. Hirao, Z. Liu, and B. Chen, Significant improvement in Mn_2O_3 transition metal oxide electrical conductivity via high pressure, Sci. Rep. **7**, 44078 (2017).

[11] J.-P. Rueff, C.-C. Kao, V. V. Struzhkin, J. Badro, J. Shu, R. J. Hemley, and H. K. Mao, Pressure induced high-spin to low-spin transition in FeS evidenced by x-ray emission spectroscopy, Phys. Rev. Lett. **82**, 3284 (1999).

[12] J.-F. Lin, G. Vankó, S. D. Jacobsen, V. Iota, V. V. Struzhkin, V. B. Prakapenka, A. Kuznetsov, and C.-S. Yoo, Spin transition zone in Earth's lower mantle, Science **317**, 1740 (2007).

[13] A. Mattila, J.-P. Rueff, J. Badro, G. Vankó, and A. Shukla, Metal-ligand interplay in strongly-correlated oxides: A parametrized phase diagram for pressure induced spin transitions, Phys. Rev. Lett. **98**, 196404 (2007).

[14] R. S. Kumar, Y. Zhang, Y. Xiao, J. Baker, A. Cornelius, S. Veeramalai, P. Chow, C. Chen, and Y. Zhao, Pressure induced high spin-low spin transition in fese superconductor studied by

x-ray emission spectroscopy and *ab initio* calculations, Appl. Phys. Lett. **99**, 061913 (2011).

[15] J.-P. Rueff, V. Balédent, K. Higashi, and H. Kageyama, Spin transition in SrFeO$_2$ under pressure by x-ray spectroscopy, Phys. Rev. B **102**, 235138 (2020).

[16] M. P. Pasternak, G. K. Rozenberg, G. Y. Machavariani, O. Naanan, R. D. Taylor, and R. Jeanloz, Breakdown of the Mott-Hubbard state in Fe$_2$O$_3$: A first order insulator-metal transition with collapse of magnetism at 50 GPa., Phys. Rev. Lett. **82**, 4663 (1999).

[17] G. Peng, F. M. F. DeGroot, K. Haemaelaeinen, J. A. Moore, X. Wang, M. M. Grush, J. B. Hastings, D. P. Siddons, and W. H. Armstrong, High-resolution manganese x-ray fluorescence spectroscopy. Oxidation-state and spin-state sensitivity, J. Am. Chem. Soc. **116**, 2914 (1994).

[18] T. A. Tyson, Q. Qian, C.-C. Kao, J.-P. Rueff, F. M. F. de Groot, M. Croft, S. W. Cheong, M. Greenblatt, and M. A. Subramanian, Valence state of Mn in Ca-doped LaMnO$_3$ studied by high-resolution Mn $K\beta$ emission spectroscopy, Phys. Rev. B **60**, 4665 (1999).

[19] S. Limandri, S. Ceppi, G. Tirao, G. Stutz, C. Sánchez, and J. Riveros, High resolution study of kβ' and k$\beta_{1,3}$ x-ray emission lines from Mn-compounds, Chem. Phys. **367**, 93 (2010).

[20] M. A. Beckwith, M. Roemelt, M.-N. Collomb, C. DuBoc, T.-C. Weng, U. Bergmann, P. Glatzel, F. Neese, and S. DeBeer, Manganese kβ x-ray emission spectroscopy as a probe of metal-ligand interactions, Inorg. Chem. **50**, 8397 (2011).

[21] M. Rovezzi and P. Glatzel, Hard x-ray emission spectroscopy: A powerful tool for the characterization of magnetic semiconductors, Semicond. Sci. Technol. **29**, 023002 (2014).

[22] S. Lafuerza, A. Carlantuono, M. Retegan, and P. Glatzel, Chemical sensitivity of Kβ and Kα x-ray emission from a systematic investigation of iron compounds, Inorg. Chem. **59**, 12518 (2020).

[23] A. D. Chijioke, W. J. Nellis, A. Soldatov, and I. F. Silvera, The ruby pressure standard to 150 GPa, J. Appl. Phys. **98**, 114905 (2005).

[24] U. Bergmann, M. M. Grush, C. R. Horne, P. DeMarois, J. P. Penner-Hahn, C. F. Yocum, D. W. Wright, C. E. Dubé, W. H. Armstrong, G. Christou *et al.*, Characterization of the Mn oxidations states in photosystem II by $K\beta$ x-ray fluorescence spectroscopy, J. Phys. Chem. B **102**, 8350 (1998).

[25] I.-H. Hwang, S. D. Kelly, M. K. Y. Chan, E. Stavitski, S. M. Heald, S.-W. Han, N. Schwarz, and C.-J. Sun, The *AXEAP2* program for $K\beta$ x-ray emission spectra analysis using artificial intelligence, J. Synchrotron Radiat. **30**, 923 (2023).

[26] P. Wang, S.-C. Zhu, Y. Zou, H. Chen, Y. Liu, W. Li, J. Chen, J. Zhu, L. Wu, S. Wang *et al.*, Concurrent pressure-induced spin-state transitions and Jahn–Teller distortions in MnTe, Chem. Mater. **34**, 3931 (2022).

[27] B. Yue, F. Hong, N. Hirao, R. Vasin, H. R. Wenk, B. Chen, and H. K. Mao, A simple variant selection in stress-driven martensitic transformation, Proc. Natl. Acad. Sci. USA **116**, 14905 (2019).

[28] J.-P. Rueff, A. Shukla, A. Kaprolat, M. Krisch, M. Lorenzen, F. Sette, and R. Verbeni, Magnetism of Invar alloys under pressure examined by inelastic x-ray scattering, Phys. Rev. B **63**, 132409 (2001).

[29] G. Vankó, T. Neisius, G. Molnar, F. Renz, S. Karpati, A. Shukla, and F. M. F. de Groot, Probing the 3d spin momentum with x-ray emission spectroscopy: The case of molecular-spin transitions, J. Phys. Chem. B **110**, 11647 (2006).

[30] M. Retegan, Crispy: v0.7.4 (2019)

[31] F. Aguado, F. Rodriguez, and P. Núñez, Pressure-induced Jahn-Teller suppression and simultaneous high-spin to low-spin transition in the layered perovskite CsMnF$_4$, Phys. Rev. B **76**, 094417 (2007).

[32] See Supplemental Material at http://link.aps.org/supplemental/10.1103/PhysRevB.111.035122 for complementary multiplet XES calculations on the influence of the crystal field parameter in *Oh* and *D4h* symmetry.

[33] H. Bilz, G. Benedek, and A. Bussmann-Holder, Theory of ferroelectricity: The polarizability model, Phys. Rev. B **35**, 4840 (1987).

[34] B. Wang, L. You, P. Ren, X. Yin, Y. Peng, B. Xia, L. Wang, X. Yu, S. Mui Poh, P. Yang *et al.*, Oxygen-driven anisotropic transport in ultra-thin manganite films, Nat. Commun. **4**, 2778 (2013).

[35] M. Baldini, T. Muramatsu, M. Sherafati, H. kwang Mao, L. Malavasi, P. Postorino, S. Satpathy, and V. V. Struzhkin, Origin of colossal magnetoresistance in LaMnO$_3$ manganite, Proc. Natl. Acad. Sci. USA **112**, 10869 (2015).